UNUSUAL RADAR ECHOES FROM THE GREENLAND ICE SHEET

E. J. Rignot, S. J. Ostro, J. J. van Zyl, and K. C. Jezek†

Jet Propulsion Laboratory, California Institute of Technology
Pasadena, CA 91109-8099

†Byrd Polar Research Center, Ohio State University
Columbus, 01143210

Airborne radar images of part of the Greenland ice sheet reveal icy terrain whose radar properties are unique among radar-studied terrestrial surfaces but resemble those of Jupiter's icy Galilean satellites. The 5.6- and 24-centimeter-wavelength echoes from the Greenland percolation zone, like the 3.5- and 13-centimeter-wavelength echoes from the icy satellites, are extremely intense and have anomalous circular and linear polarization ratios. However, the detailed subsurface configurations of the satellite regoliths, where heterogeneities are the product of prolonged meteroid bombardment, are unlikely to resemble that within the Greenland percolation zone, where heterogeneities are the product of seasonal melting and refreezing.

Submitted to Science, April 27, 1993.

Revised July 26, 1993.

It has been known since the 1970's that radar echoes from the icy Galilean satellites are extraordinary (1). The radar reflectivities (2) of Europa, Ganymede, and Callisto are several orders of magnitude greater than those recorded for comets, the Moon, the inner planets, and nonmetallic asteroids, and show little dependence on the radar wavelength. In addition, the satellites' circular polarization ratios μ_C (3) exceeds unity, whereas μ_C is less than 0.4 for most other planetary targets, and their linear polarization ratios μ_L are about 0.5, again larger than values for other planets (4). More recently, radar observations of the Mars residual south polar ice cap (5), portions of Titan (6), and polar caps on Mercury (7) have revealed that surfaces with high radar reflectivity and μ_C >1 exist elsewhere in the solar system.

Here we report the measurement of similarly exotic radar signatures for icy surfaces on Earth. The observations were collected in June 1991 by the NASA/Jet Propulsion laboratory airborne synthetic-aperture radar (AIRSAR) instrument above a vast portion of the Greenland ice sheet called the percolation zone (Fig. 1), where summer melting generates water that percolates down through the cold, porous, dry snow and then refreezes in place to form massive layers and pipes of solid ice (8). The radar observations were collected simultaneously at 5,6-, 24-, and 68-cm wavelengths, and the complete scattering matrix (9) of each resolution element was measured at each radar wavelength. At the time of the radar flight, ground teams recorded the snow and firn (old snow) stratigraphy, grain size, density, and temperature (1 O) at ice camps in three of the four snow zones identified by glaciologists to characterize four different degrees of summer melting (8).

Figure 2 shows average values of the radar reflectivity σ^0_{RL} (2), the circular polarization ratio μ_C, and the linear polarization ratio μ_L obtained from AIRSAR measurements at the Crawford Point site in the percolation zone. At 5.6 and 24 cm, σ^0_{RL} is higher than unity at 18°, decreases toward higher incidence angles, and shows few spatial features. At 68 cm, σ^0_{RL} is ten times lower, but shows kilometer-scale spatial variations. μ_C is larger than unity at 5.6 and 24 cm for incidence angles larger than 30° and 45o, respectively, increasing to 1.6 and 1.4 at 66°. At 68 cm, μ_C is everywhere less than 0.8 and drops as low as 0.1 in some places, with kilonmtcr-scale spat ial variations negat ivel y correlated with those observed in t he radar reflectivit y images. μ_L is as large as 0.46 at 5.6 cm and 0.22 at 24 cm, but remains less than 0.1 at 68 cm.

In the AIRSAR scenes of the Swiss camp and the GISP 11 sites, at all three wavelengths, corresponding values of σ^0_{RL} are 10 to 30 times lower than at Crawford Point; μ_C is less than 0.4, and μ_L is less than 0.1. To the best of our know] edge, no natural terrestrial surface other than the Greenland percolation zone shows strong echoes with $\mu_C > 1$ and $\mu_L > 0.3$ (10). However, strong cc} 1ocs with large values of μ_C and μ_L have been reported for the icy Galilean satellites.

Figure 3 shows mean values of disk-integrated radar reflectivities σ^0_{OC} and circular polarization ratios μ_C for Europa, Ganymede, Callisto, and the Moon, and corresponding quantities for Greenland obtained by averaging σ^0_{RL} and μ_C over the Crawford Point scene. The figure shows that the average radar properties of the percolation zone at 5.6 and 24 cm (average $\mu_C > 1$, large reflectivity) resemble those of the icy satellites at 3.5 and 13 cm. 1 lowever, Greenland's average values at 24 cm arc several tens of percent lower than at 5.6 cm, and $\mu_C < 1$ at 68 cm, indicating a change in the scattering process at the longer wavelengths, whereas 70-cm estimates of μ_C for the icy satellites apparently exceed unity (12). Also, μ_C for the percolation zone decreases significantly from 66^o to 18^o, whereas no such difference has been noticed for the icy satellites (see Fig. 3 caption); and σ^0_{RL} is a much stronger function of the incidence angle than in the case of the icy satellites.

Several years ago, Zwall y (13) suggested that icc inclusions could explain low emissivities measured for the percolation zone by spaceborne microwave radiometers. Since then, surface-based radio sounding experiments, and airborne active and passive microwave measurements (14), have supported the hypothesis that volume scattering from subsurface ice layers and ice pipes is the major influence on the radar returns. Recent surface-based radar observations conducted at Crawford Point (10) at 5.4 and 2,2 cm further indicate that, at incidence angles between 10° and 70°, most of the scattering takes place in the most recent annual layer of buried ice bodies.

Figure 4 shows a representative example of firn stratigraphy in the percolation zone in early summer. Ice bodies generated from a previous summer melt are found 1.8 m below the surface. Ice layers, a millimeter to a few centimeters thick, extend at least several tens of centimeters across, parallel to the firn strata (8). Ice pipes, several centimeters thick and several tens of centimeters long, are vertically extended masses reminiscent of the percolation channels that conduct melt water down through the snow during summer, feeding ice layers. The fact that radar returns measured at 68 cm are significantly weaker and have lower polarization ratios than those at 5.6 and 24 cm suggests that the discrete scatterers responsible for the radar echoes are of typical dimension less than a few tens of centimeters, similar to the scales of the solid-ice inclusions. The 68-cm echoes probably are dominated by single reflections from deeply buried layers of denser firn or concentrated ice bodies, whereas the 5.6- and 24-cm echoes probably are dominated by multiple scattering from the ice layers and pipes in the most recent annual layer. The relatively sharp decrease in μ_C and μ_L for θ less than 40° perhaps reveals the presence of a strong, specular reflection from the ice layers at small incidence angles, which is also suggested by the strong dependence of radar reflectivity on incidence angle.

Ice layers and pipes also form in the soaked zone, but the snow there is so saturated with liquid water that the radar signals are strongly attenuated, cannot interact with the buried ice formations, and hence yield echoes with low reflectivities and polarization ratios. In the dry-snow zone, the snow is dry, cold, porous, clean, and therefore very transparent at microwave frequencies, but does not contain solid-ice scatterers that could interact with the radar signals.

For the satellites, no in-situ measurements exist or are planned, but theoretical interpretations favor subsurface volume scattering as the source of the radar signatures. Hapke (15) suggested that the mechanism responsible for the satellites' radar behavior is the coherent backscatter effect, also known as weak localization (16), which has been observed in laboratory-controlled experiments of scattering of light from weakly absorbing, disordered random media. Coherent backscattering can theoretically produce strong echoes with μ_C >1 (the helicity of the incident polarization is preserved through multiple forward scattering) and $\mu_L \approx$ 0.5, provided that (i) the scattering heterogeneities arc comparable to or larger than the wavelength (1 7), and (ii) the relative refractive index of the discrete, wavelength-sized scatterers is smaller than 1.6 (Fig. 9 of (18)). As noted by Ostro and Shoemaker (19), prolonged impact cratering of the satellites probably has led to the development of regoliths similar in structure and particle-size distribution to the lunar regolith, but the high radar transparency of ice compared with that of silicates permits longer photon path lengths, and higher-order scattering. Hence coherent back scatter can dominate the echoes from Europa, Ganymede, and Callisto, but contributes negligibly to lunar echoes. Similarly, the upper few meters of the Greenland percolation zone arc relatively transparent (unlike the soaked zone) and, unlike the dry-snow zone, contain an abundance of solid-ice scatterers at least as large as the radar wavelength, with a relative refractive index of about 1.3, so coherent backscatter also can dominate the echoes there. However, the detailed subsurface configurations of the satellite regoliths, where heterogenei t ics arc the product of meteoroid bombardment, seem unlikely to resemble that within the Greenland percolation zone, where heterogeneities are the product of seasonal melting and freezing.

Wc conclude that a variety of natural subsurface configurations can yield exotic radar properties, Given the increasing number of solar system surfaces (5,6,7) characterized by high radar reflectivities and polarization ratios, it is desirable to define as accurately as possible the physical constraints provided by the radar measurements. The Greenland percolation zone constitutes a uniquely accessible, n at ura] laboratory for studying exotic radar scattering processes in a geological setting. Direct sampling and high-resolution, multi-wavelength radar imaging of that terrain could reveal the detailed relationship between radar signature and subsurface configurate ion, thereby furnishing a modicum of ground truth for interpreting echoes from extraterrestrial surfaces.

REFERENCES AND NOTES

1. S. J. Ostro *et al., J. Geophys. Res.* 97, 18277 (1 992).

2. Radar reflectivity σ^0 equals 4π times the backscattered power per steradian for unit incident flux at the target, divided by the target's projected area. Radar reflectivities for the icy Galilean satellites are mean values of disk-integrated measurements. Radar reflectivities measured by AIRSAR are single-pixel values.

3. Echoes in the same circular (SC) polarization are obtained by transmitting and receiving right circular or by transmitting and receiving left circular. That is, SC denotes either RR or LL, where R and L stand for right and left. Similarly, OC denotes either RL (right circular transmitted and left circular received) or LR. Specular reflection from a smooth surface reverses the helicity of circular polarization but preserves tile direction of linear polarization. The circular and linear polarization ratios (μ_C = SC/OC, i.e., RR/RL or 1,1,/1,1{; and $\mu_L = OL/SL$, where SL means same linear), of echo power in orthogonal senses, are defined so they equal zero for backreflect ion from a perfect 1 y smooth dielectric interface. Linear polarization ratios measured by AIRSAR are computed using μ_L = JIV/Jill, where 11 and V stand for horizontal and vertical.

4. S. J. Ostro, 1). B. Campbell, G. II. Pettengill, and I. I. Shapiro, *Icarus* 44, 431, (1980).

5. D. O. Muhleman, B. J. Butler, A. W. Grossman, and M. A. Slade, Science 253, **1508 (1991).**

6. D. O. Muhleman, A. W. Grossman, B. J. Butler, and M. A. Slade, *Science* 248,

9'75 (1990); D. O. Muhleman, A. W. Grossman, M. A. Slade, and B. J. Butler, *Bull. Am. Astron. Sot.* *24, 954 (1992).*

7. M. A. Slade, B. J. Butler, and D. O. Muhleman, Science 258, 635 (1992); J. K. Harmon, and M. A. Slade, *Science 258, 640 (1992).*

8. C. S. Benson, US Army Snow Ice Permafrost Res. Estab. Res. Rep. 70 (Hanover, NH, 1962).

9. J. J. van Zyl and F. T. Ulaby, in *Radar Polarimetry for Geoscience Applications,* *F.* Ulaby and C. Elachi, Eds. (Artech House, Norwood, MA, 1990), Chap. 2.

10. K. C. Jezek and S. P. Gogineni, *IEEE Geosc. Rem. Sens. Sot. Newsletter 85, 6 (1992),*

11. Double reflections from the dihedral reflectors formed by city buildings or flooded trees yield strong radar echoes, with μ_C >1 (each reflection reverses the helicity of the polarization), but μ_L (here either HV/HH or VH/VV) is close to zero (9). Surface scattering from surfaces of rms height comparable to or larger than the radar wavelength, such as rough lava flows (J. J. van Zyl, C. F. Burnette, and q'. G. Farr, *Geophys. Res. Lett.* 18, 1787 (1991)), yields σ^0_{RL} <0,2, μ_C <0.4, and μ_L < 0.2 at all three wavelengths, for θ = 30°. Volume scattering from heavily vegetated areas, such as tropical rain forest (A. Freeman, S. Durden, and R. Zimmerman, Proceedings of the International Geoscience and Remote Sensing Symposium, Houston, Texas, May 26-29, 1992, IEEE New York Pub., 1686 (1992)), yields $\mu_C \approx 1$ and $\mu_L \approx$ 0.3 at 24 and 68 cm, $\mu_C \approx$ 0.8 and $\mu_L \approx$ 0.25 at 5.6 cm, but σ^0_{RL} < 0.1 at all three wavelengths, for O = 55°. Unlike Greenland, none of these objects show very strong echoes with large polarization ratios.

12. 11.11. Campbell, R. A. Simpson, and S. J. Ostro, unpublished.

13. H. J. Zwally, *J. Glaciol.* 18, 195 (1977),

14. C. T. Swift, P. S. Hays, J. S. Herd, W, L. Jones, and V, E. Delmore, *J. Geophys. Res.* **90, 1983 (1985).**

15. B. Hapke, *Icarus* 88, 407 (1990).

16. F. C. Mackintosh and S. John, *Phys.* Rev. *B* 37, 1884 (1988); M. 1'., van Albada, M. B. van der Mark and A., Lagendijk, in *Scattering and localization of Classical Waves in Random Media, P.* Sheng, Ed. (World Scientific, Singapore, 1990), p. 97, and references therein.

17. K. J. Peters, *Phys. Rev.* B **46**, 801 (1992).

18. M. I. Mishchenko, *Earth, Moon, and Planets 58, 127 (1 992).*

19. S. J. Ostro and E. M. Shoemaker *Icarus* 85, 335 (1990). In contrast to the case of Ganymede and Callisto, few impact craters have been identified on Europa, and it is not clear whether the surficial layer of Europa is generated primarily by impacts or by internal processes, such as frost deposition.

20, Wc thank Dr. R.. Thornas, Head of the Polar Research Program at NASA Headquarters, for supporting this research; the people from the AIRSAR team for collecting and processing of the SAR data used in this manuscript; Mr. J. Crawford for coordinating the AIRSAR overflights; and Drs. P. Gogineni and M. Drinkwater for discussions about Greenland glaciology. Part of this work was carried out at the Jet]'repulsion Laboratory, California Institute of Technology, under contract with the National Aeronautics and Space Administration.

FIGURE CAPTIONS

Figure 1. Map of Greenland showing the four snow zones defined by Benson (8), the flight track of AIRSAR (continuous thick line), and the location of the Swiss Camp, Crawford Point, and the GISP II sites. Melting rarely occurs in the dry-snow zone; forms massive, buried, solid-ice inclusions in the percolation zone; saturates the snow with liquid water in the soaked zone; and removes the seasonal snow cover and ablates the glacier ice in the ablation zone.

Figure 2. Average values of the (A) OC radar reflectivity σ^0_{RL}, (B) circular polarization ratio $\mu_C = \sigma^0_{RR}/\sigma^0_{RL}$, and (C) linear polarization ratio $\mu_L = \sigma^0_{HV}/\sigma^0_{HH}$ for the Greenland percolation zone obtained by averaging the radar measurements recorded by AIRSAR at Crawford Point along the flight path, at 5,6, 24, and 68 cm, as a function of the incidence angle of the radar illumination, θ.

Figure 3. Disk-integrated average radar properties. Points for extraterrestrial targets arc averages of disk-integrated measurements at various subradar longitudes (Fig. 10 of (1)). Disc-resolved echo spectra, which are equivalent to brightness scans through a slit parallel to the projected spin vector, show hardly any variation in μ_C across the satellite discs (Fig. 2 and 3 of (1)). For Greenland, points are averages of measurements that span incidence angles, θ, from 18° to 66°. 10% of the projected area is at $\theta \leq$ 18°, and 17% is at $\theta \geq$ 66°.

Figure 4. Snow stratigraphy at Crawford Point on the day of the AIRSAR observations. Snow grain diameters arc less than 1 mm in fine-grained snow and more than 1 mm in coarse- grained snow. The average snow density is 0.2 g/cm^3 in the top 40 cm and 0.4 g/cm^3 between 40 and 200 cm. Wind crusts arc paper-thin

layers of firmly bonded, fine-grained snow. Depth hoar consists of large, skeletal crystals formed in snow strata by crystallization directly from water vapor when a temperature gradient exists in the snow.

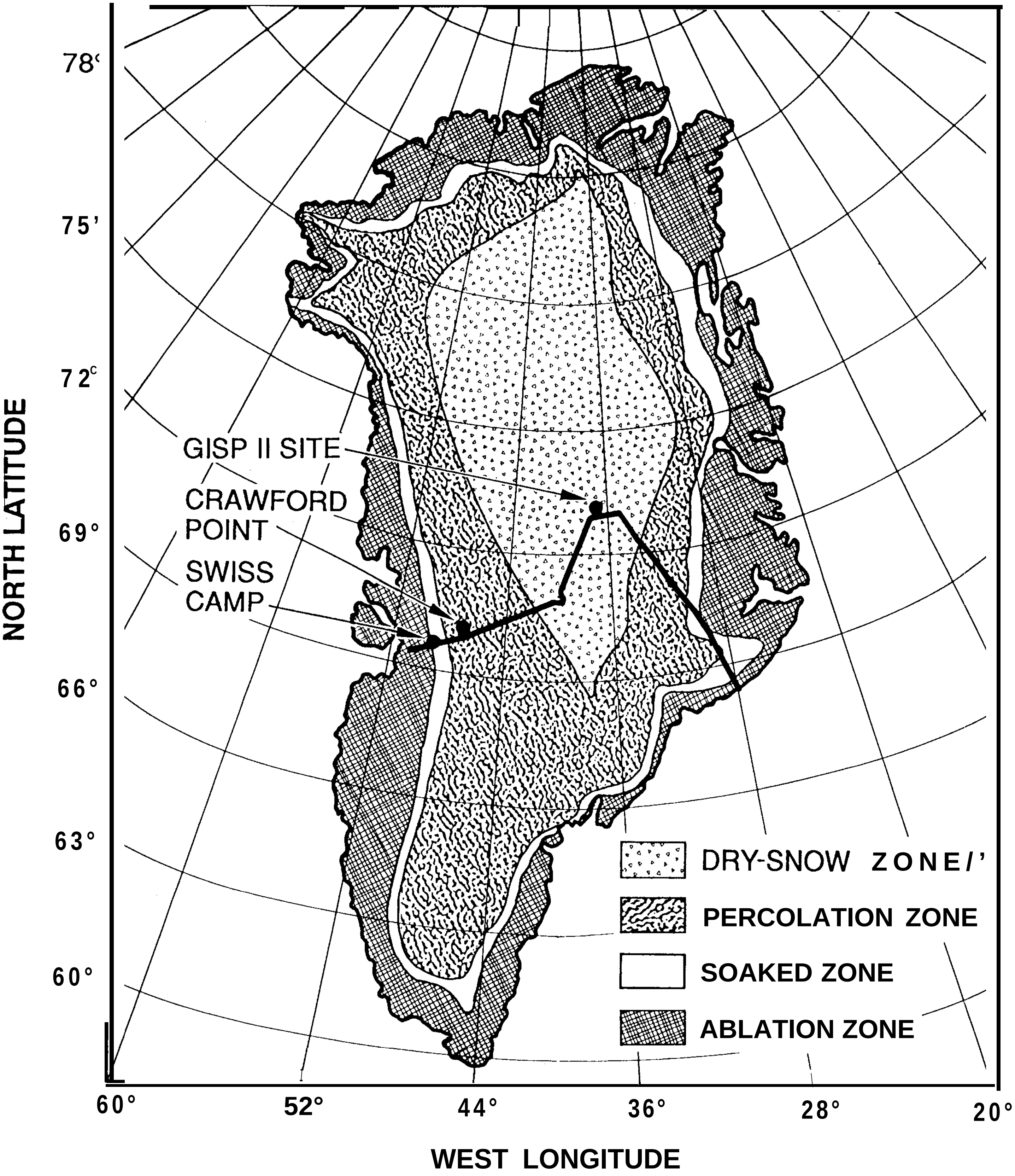

78°
75°
72°
69°
66°
63°
60°
NORTH LATITUDE
GISP II SITE
CRAWFORD POINT
SWISS CAMP
DRY-SNOW ZONE
PERCOLATION ZONE
SOAKED ZONE
ABLATION ZONE
60°
52°
44°
36°
28°
20°
WEST LONGITUDE

Rignot, Fig. 1

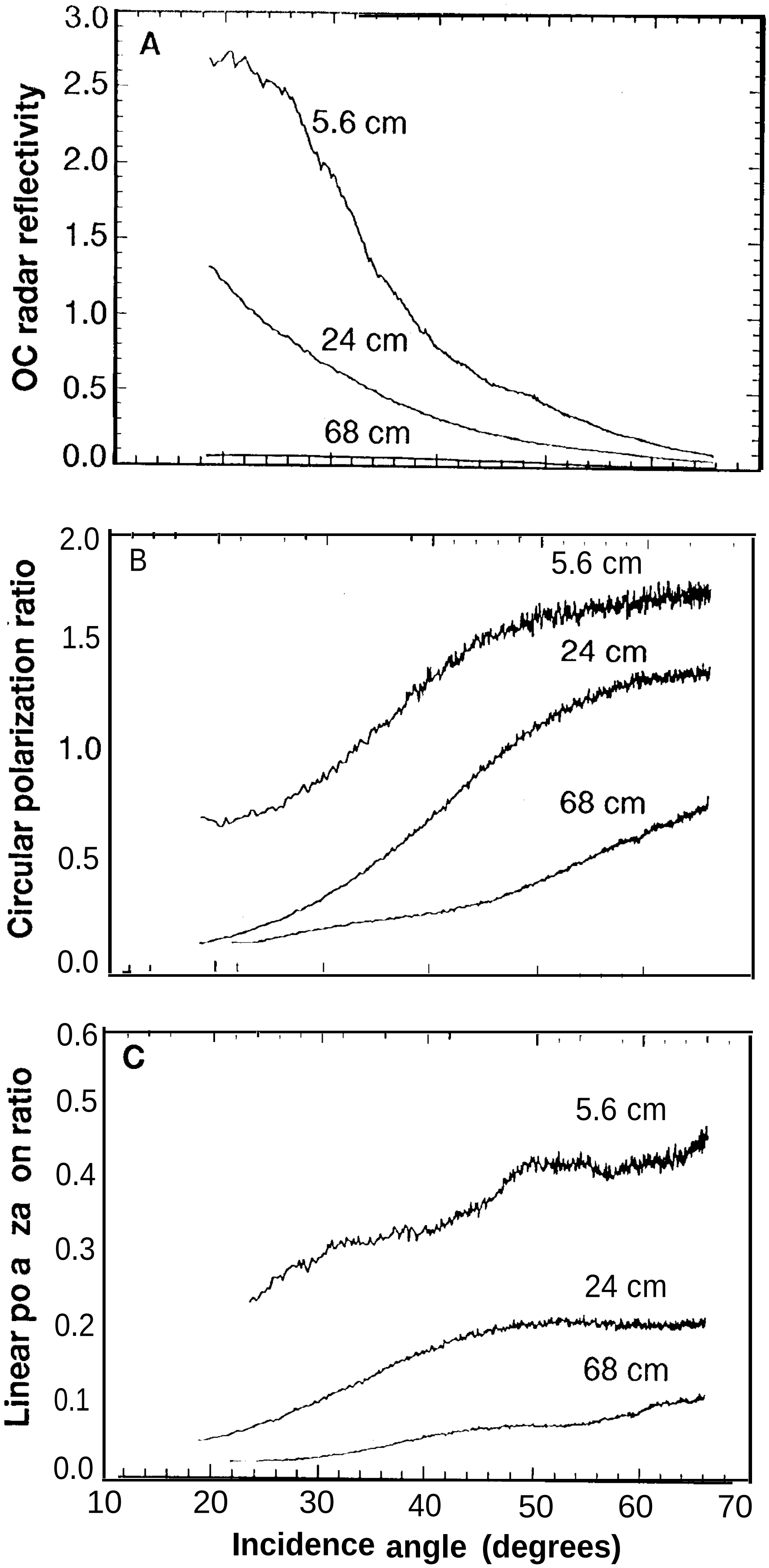
A
OC radar reflectivity
5.6 cm
24 cm
68 cm
B
Circular polarization ratio
5.6 cm
24 cm
68 cm
C
Linear po a za on ratio
5.6 cm
24 cm
68 cm
Incidence angle (degrees)

Rignot, Fig. 2

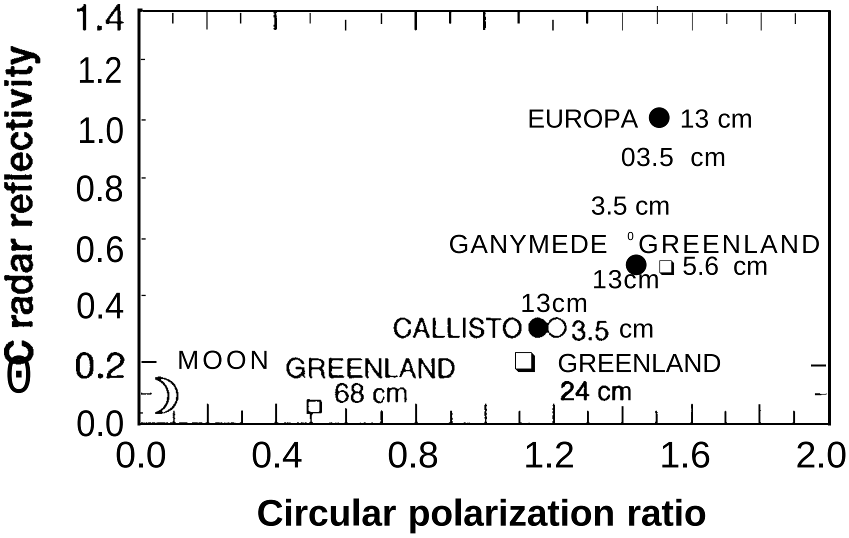

1.4
1.2
1.0
0.8
0.6
0.4
0.2
0.0
radar reflectivity
EUROPA
13 cm
03.5 cm
3.5 cm
GANYMEDE
GREENLAND
13cm
5.6 cm
13cm
CALLISTO
3.5 cm
MOON
GREENLAND
68 cm
GREENLAND
24 cm
0.0
0.4
0.8
1.2
1.6
2.0
Circular polarization ratio

Rignot, Fig. 3

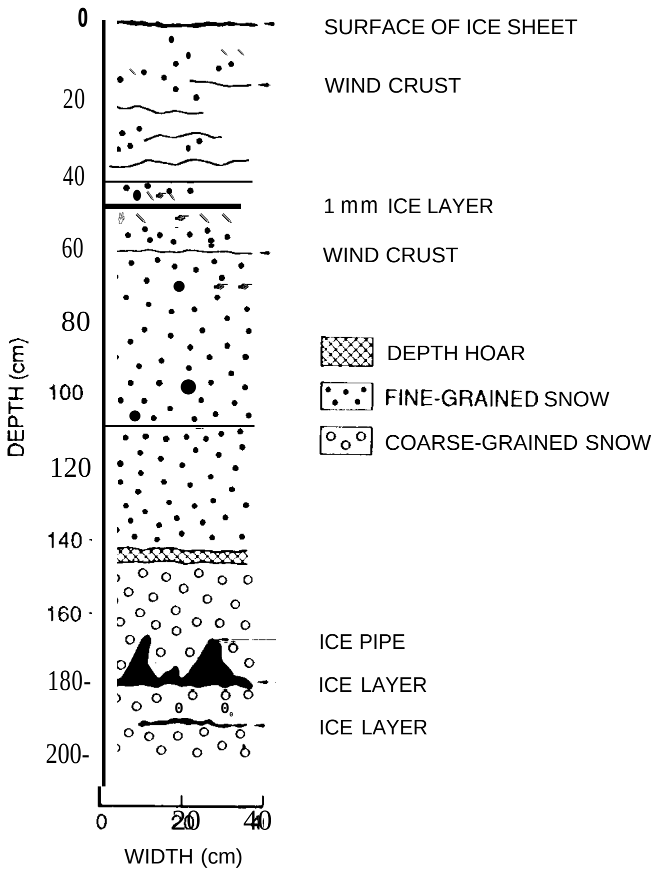

0
20
40
60
80
100
120
140
160
180
200
DEPTH (cm)
0
20
40
WIDTH (cm)
SURFACE OF ICE SHEET
WIND CRUST
1 mm ICE LAYER
WIND CRUST
DEPTH HOAR
FINE-GRAINED SNOW
COARSE-GRAINED SNOW
ICE PIPE
ICE LAYER
ICE LAYER

Rignot, Fig. 4